

Remote Sensing of Atmospheric Turbidity Variation by Satellite

ALDEN McLELLAN*

*Space Science and Engineering Center
University of Wisconsin, Madison, Wis.*

1. Introduction

IN recent years a number of scientists from various disciplines have stated that the Earth's atmospheric mean temperature in this century is directly related to man's actions which have altered the carbon dioxide and particulate matter content of the atmosphere (see for example, Risebrough, Huggett, Griffin, and Goldberg,¹ Davitaya,² Bryson and Wendland,³ Bryson⁴). This conclusion concerning particulate loading was obtained from 50-year data on urban smoke-haze days, turbidity factors from incidence radiation data in Hawaii, dust fall in the Caucasus Mountains in Russia, and the transport of DDT pesticides across the Atlantic Ocean by means of the northeast trade winds. On the other hand, the thesis has been put forward that man's activities have had very little to do with the global increase in dust loading of the atmosphere, but rather that this phenomena is due to natural processes, such as winds over arid land masses and volcanic activity, which has been rapidly increasing over the past quarter of a century (Mitchell,^{5,6} Manabe and Wetherald⁷).

It has been shown by Atwater (1970) that the absorption and scattering by aerosols of solar radiation along with the reflective properties of the surface underneath determine the albedo of the region. A change in the albedo, which can be caused by a variance in the particulate loading of the atmosphere, results in atmosphere heating and cooling even at surface levels (McCormick and Ludwig⁹). Small changes in particulate loading or in the type of particulate, such that the ratio of absorption to scattering changes, can reverse heating or cooling trends (Charlson and Pilat¹⁰).

In this Note we direct our attention to the solar radiation absorbed and reflected from the atmospheric particulates over an urban area. Thus, we are primarily concerned with the urban albedo, the feasibility of monitoring this man-made particulate pollution, and the possible long term effects. The addition of particulate loading or a change in the type of particulate will modify the backscattering and absorption of solar radiation, therefore, it will alter the albedo. If we consider the total albedo A in two component parts, we have

$$A = \text{Area Averaged } (A_s + A_a) \quad (1)$$

where A_s is the albedo of the surface alone, and A_a is that part due to the atmosphere. In most situations in which there occurs an increase in pollution or dust, it can be correctly assumed that the backscattering increases also, thereby increasing A_a (McCormick and Ludwig⁹). However, there

are situations which are not uncommon where an increase in pollution or dust will cause a decrease in A_a (Charlson and Pilat¹⁰). Such is the case considered here.

Since there has been no satellite launched which has as its primary objective the detection of local air pollution, or for that matter even global pollution, it therefore seemed reasonable to determine the possibility of observing local atmospheric turbidity from an operating satellite with optical detectors aboard for sensing the entire Earth's disk, even though these detectors were not primarily designed for haze observation (McLellan¹¹). It is shown in this work that the reflected visible radiation from the city of Los Angeles as received by the geosynchronous Applications Technology Satellite (ATS) III at 40 min intervals on April 23, 1968 can be successfully correlated with various ground based data. Robinson and Drummond¹² have pointed out that a bright land area, such as the urban section of Los Angeles considered here, which has a relatively high surface albedo, A_s , may appear darker when seen from above when the atmosphere is polluted with particulates that are absorbing and have little backscatter. The analysis of the data indicate that the atmospheric turbidity decreased throughout this particular day as the outgoing visible radiation increased. It is implied from the success of this initial step that atmospheric turbidity variation monitoring over global, as well as local, regions is possible by proper data analysis from remote sensing satellites (McLellan¹³).

2. The Satellite and Camera System

The Applications Technology Satellite III (ATS-III) is the third of a series of ATS scientific satellites built for NASA Goddard Space Flight Center (Darcy¹⁴). The ATS-III is a cylinder with its spin stabilized at a nominal 100 rpm and its spin axis aligned with that of the Earth. Two independent thrust control jet subsystems are used for adjustments in orbital inclination and eccentricity. The satellite is at Earth synchronous height of 35,000 km. Two ground stations track and control the spacecraft, conduct experiments, and record and process spacecraft data. The controlling ground station at Rosman, N.C. assumes primary responsibility for the data acquisition from the Multicolor Spin Scan Cloud Camera (MSSCC). Data for this Note was processed directly from the primary digital tapes recorded at the ground station. The subsatellite point on April 23, 1968 was located over the equator at 60° W long.

The MSSCC consists of a high resolution telescope, three photomultiplier light detectors, and a precision latitude step mechanism. The latitude step motion, combined with the spinning motion of the ATS satellite, permits scanning a complete Earth disk with a ground resolution of about 3 km at the satellite subpoint. The MSSCC video circuitry consists of identical amplifier channels for each of the three colors, blue, green and red. However, the analysis in this Note concerns only the green channel data.

3. Observation

On April 23, 1968, nine scans of green channel data of the Earth's disk at 40 min intervals over 6 daylight hours were recorded in digital form on magnetic tape. The spectral range of the green channel photomultiplier of the Multicolor Spin Scan Camera on board the ATS-III is shown in Fig. 1. A numerically enhanced computer generated picture of a small section of the Earth's disk comprising the cloud-free southern California region is shown in Fig. 2. Los Angeles, which is located at 34° N lat and 118° W long, can be seen as the relatively bright area near the center. The Salton Sea and the islands, Santa Catalina, Santa Cruz, and San Clemente can be clearly identified for orientation and alignment purposes. The ground resolution of the spin-scan camera at this latitude is on the order of 3-4 km. Figure 3 is a data

Received April 16, 1973; revision received June 11, 1973. The author wishes to make the following acknowledgements: The National Weather Service supplied the data for visibilities taken at the Los Angeles International Airport and the Long Beach Municipal Airport; The Los Angeles County Air Pollution Control District supplied the hourly sampling data of particulate matter and molecular pollutants, which were taken at their downtown station. The work upon which this publication is based was performed pursuant to Contract 68-02-002 with the Environmental Protection Agency.

Index categories: Atmospheric, Space, and Oceanographic Sciences; Computer Technology and Computer Simulation Techniques; Earth Satellite Systems, Unmanned.

* Principal Research Scientist, Remote Sensing Group. Member AIAA.

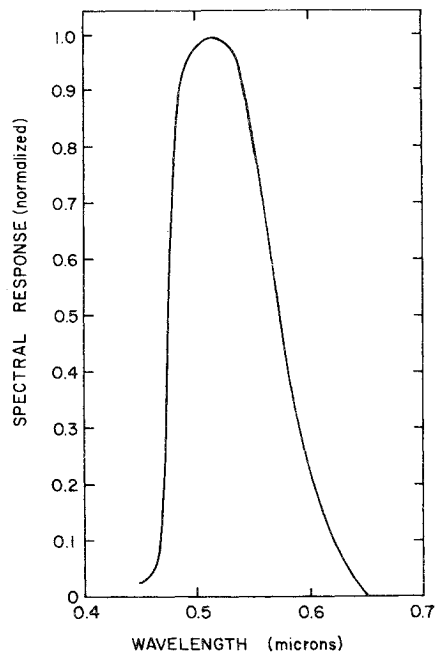


Fig. 1 Spectral response curve for the green channel of the scanning camera on board the Applications Technology Satellite III.

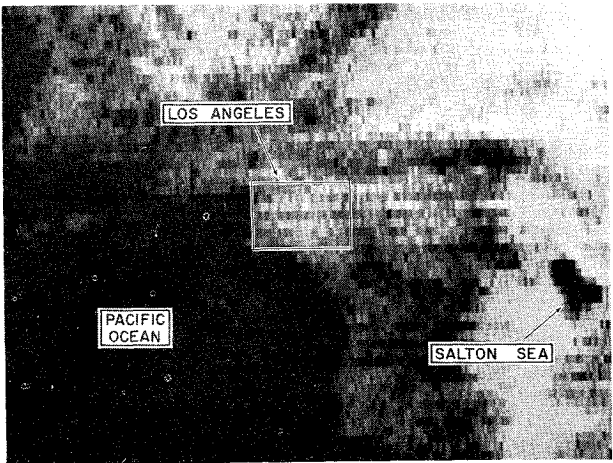


Fig. 2 Enhanced computer-generated photograph of the southern California region on April 23, 1968.

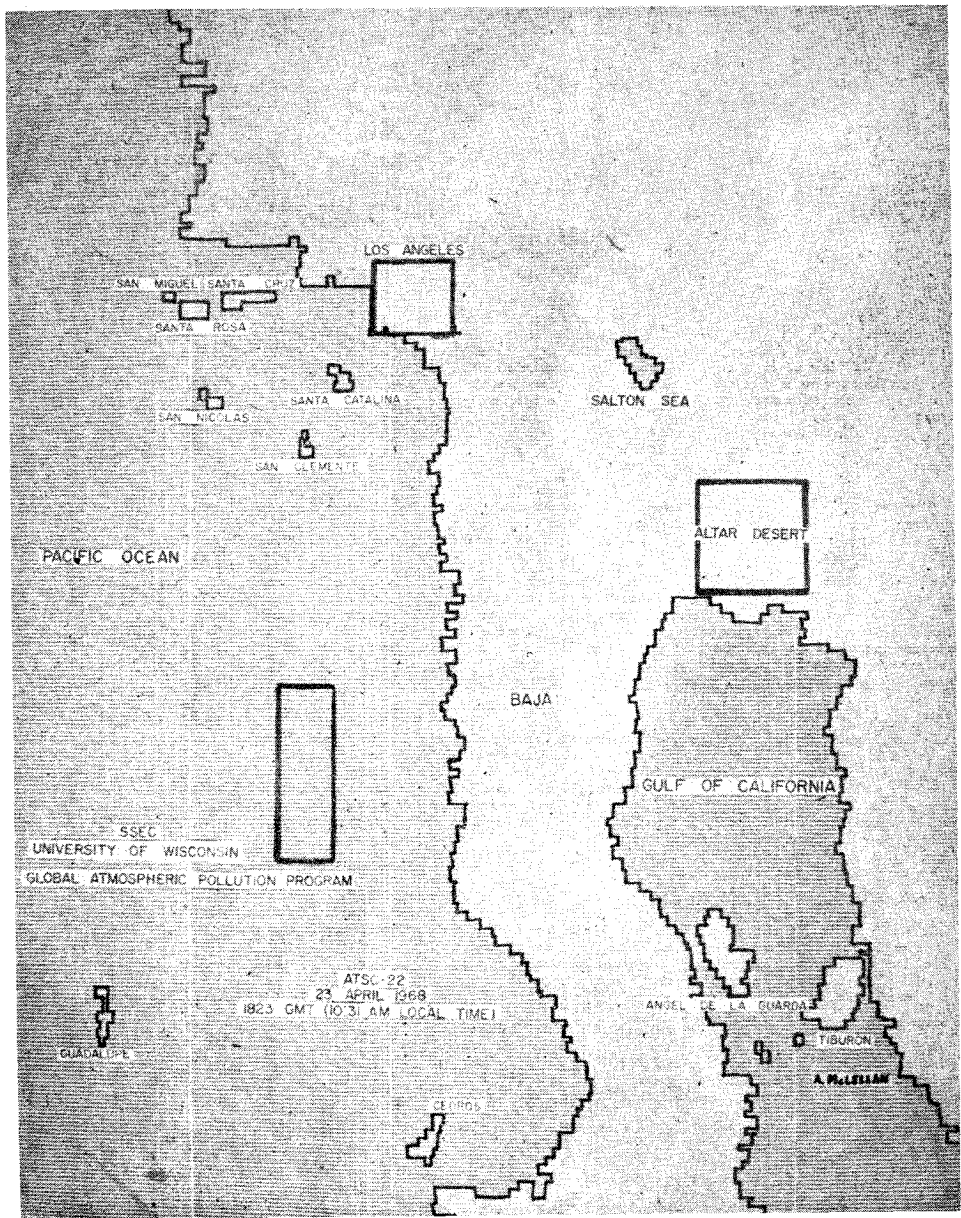


Fig. 3 Each digital radiance value for the southern California-Baja region is displayed in a form that has been modified by shading to show the three areas chosen for hourly satellite observation on April 23, 1968.

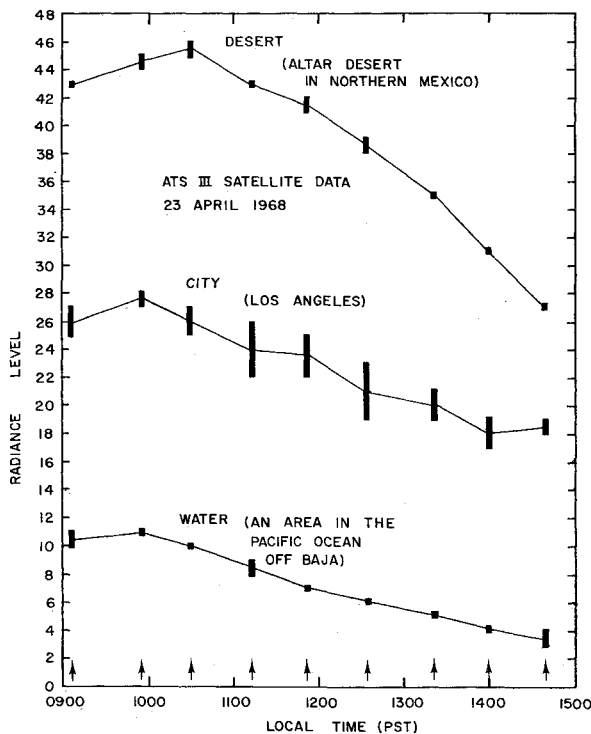


Fig. 4 Outgoing radiation from the three areas marked in Fig. 3 as observed by the ATS-III satellite.

display of each brightness value over the southern California-Baja region modified by shading for navigation purposes. Familiar landmarks such as the five small islands, San Miguel, Santa Cruz, Santa Rosa, San Nicolas, Santa Catalina, and San Clemente are clearly visible. Outlined by rectangles are the three areas chosen for satellite observation, the city of Los Angeles, the Altar Desert located north of the Gulf of California, and an area in the Pacific Ocean off the western coast of Baja.

Figure 4 shows the reflected upward green radiance from the Altar Desert (top curve), the city of Los Angeles (middle curve) and the area in the Pacific Ocean near Baja (bottom curve). Each data bar describes the range of radiance averages taken over a series of smaller areas within the overall region as marked off in Fig. 3. The hourly decrease in all curves was due to the variation in the satellite-sun angle.

A correction for the satellite-sun angle effect on the Los Angeles data was taken into account in the following way. Midrange radiance values were determined from the bright area (Altar Desert) data and the dark area (Pacific Ocean) data. The hourly percentage deviation from these means were then calculated in each case. For example, the first hour the maximum, and the last hour percentage deviation from the midrange radiance value for the two cases are given below.

The percentage deviations of both the bright and dark areas were averaged hourly and these hourly averages were used to eliminate the satellite-sun angle variations from the Los Angeles data. It was assumed that the turbidity over these

Table 1 Hourly percentage deviations

	Bright area (Altar Desert)		Dark area (Pacific Ocean)	
	Hour (PST)	Percentage deviation	Hour (PST)	Percentage deviation
First hour	0902	+22.8%	0902	+53.9%
Hour of max %	1024	+28.6%	0943	+69.3%
Last hour	1434	-22.8%	1434	-53.9%

two areas, whose albedos bracketed that of Los Angeles and whose longitude-latitude positions are near that of the city, remained constant throughout the observing hours, and that their albedos variations were due only to the varying satellite-sun angle.

It is assumed that the reflective properties of the three surfaces are of a lambertian character. The large sea surface area and the relatively large flat area of the Altar Desert were chosen, in part, because they approximate lambertian surfaces. However, a city, in general, cannot be considered as having a lambertian surface due to its linear array of vertical planes. The observations presented here cover such a large area over the Los Angeles region, where the streets tend to be randomly oriented, and where the surface resolution of each satellite data point is on the order of hundreds of buildings, that the vertical features will not present a large systematic nonlambertian reflection to account for a significant portion of the observed percentage variation in upward radiation. This fact is borne out in the small "error" bars on the radiance curve for Los Angeles in Fig. 4.

Graphed along with these "corrected" radiance values in Fig. 5 are hourly horizontal visibility data determined from the sighting of landmarks at two airports within the city and particulate matter sampling measurements of the smoke, soot, and tarry matter in the atmosphere in downtown Los Angeles. These urban pollutants are determined by a reflectometer measurement of the albedo of the deposit on a filter sample. The unit of measure, K_m (an arbitrary unit), is defined as the deposit which produces an absorbance of 0.1 when the deposit area is one square centimeter and the volume of air sampled is one cubic meter. The decrease in pollution over Los Angeles throughout this particular day (which was a reasonably clear day for Los Angeles) was caused by westerly winds from the ocean which increased steadily from 2 knots in the morning to 16 knots in the late afternoon.

Hourly decreases of three of the major Los Angeles automobile pollutants are shown in Fig. 6. This graph is typical of the daily variation of the surface concentration of these

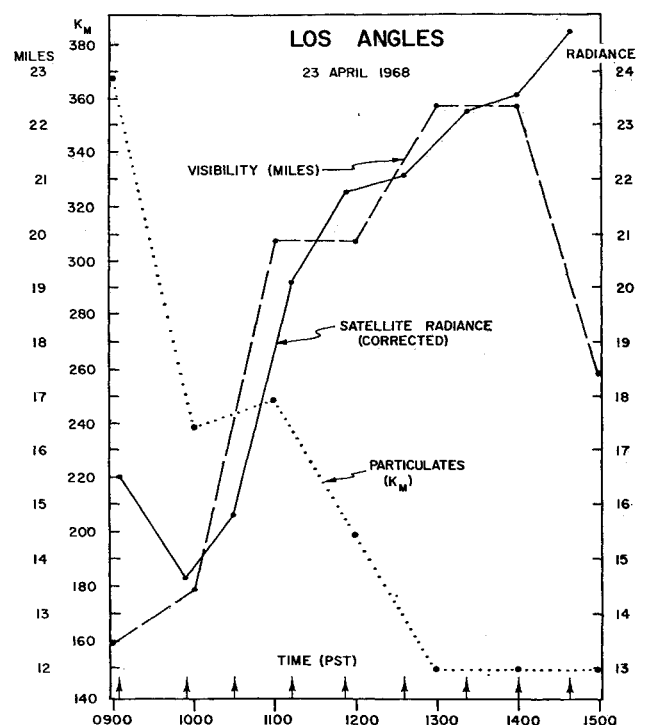


Fig. 5 A composite graph showing the relative relationships between the increasing outgoing radiation corrected for sun angle effects, increasing horizontal visibility, and decreasing particulate matter.

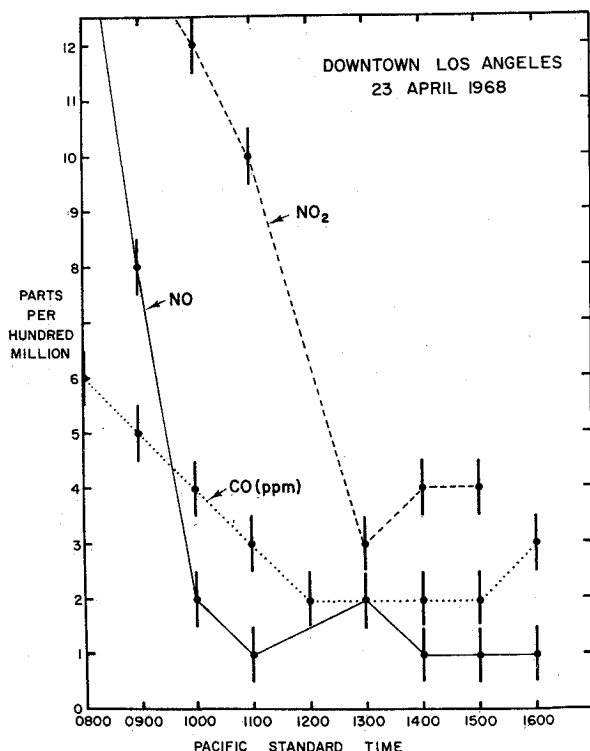


Fig. 6 The sharp morning-to-afternoon hourly decrease in the major Los Angeles molecular pollutants.

molecular pollutants, which are primarily a function of the traffic rate and the height of the mixing layer. Industrial pollution over relatively bright surface areas will tend to serve as a radiation heating mechanism rather than as a cooling mechanism, thereby enhancing the urban heat island effect (Sundborg¹⁵).

4. An Ultraviolet Observation

An analysis of the results of Nader et al.¹⁶ shows similar results for a variation in ultraviolet radiation. On Oct. 12, 1965, a moderately smoggy day over Los Angeles with downtown overcast all day, incoming and outgoing uv radiation ($0.3\text{--}0.4\mu$) was measured at hourly intervals in order to evaluate its importance in photochemical reactions. The meteorological conditions were similar to those on April 23, 1968. Wind increased from 4 mph in the morning to 8 mph from the west in the afternoon. From morning to afternoon, the particulate reflectance decreased by 85%, the polluting gases, CO, NO₂, and NO, decreased over 50%, the turbidity coefficient (McCormick and Baulch¹⁷) decreased 93%, horizontal visibility increased 130% and the upwelling uv radiation observed by aircraft at 5600–6000 ft increased 110%. However, it is interesting to note that the downward ultraviolet solar and sky irradiance ($0.3\text{--}0.38\mu$) showed a marked increase from morning to afternoon unlike our results for visible radiation. These lower morning values of uv irradiance coinciding with heavier pollution attest to the participation of ultraviolet radiation in photochemical reactions. From the results of Nader et al., the surface ultraviolet albedo, A_s , of Eq. (1), of Los Angeles was found to be about 0.15.

5. Discussion

Computations have been performed by Rasool and Schneider¹⁸ showing the effects of global temperature variations due to large increases in aerosol densities. In their results, the net effect of the increase in particulate density is to reduce the surface temperature of the Earth, because the over-all global albedo of the Earth's surface is lower than the albedo of the Earth covered with some finite amount of an "average kind" of aerosol. From this it follows that the

intensity of the upward radiation at the top of the atmosphere increases as highly reflective particulate levels increase. However, this is not the case in certain special situations. If we consider, for example, a region with a relatively large surface albedo such as a desert, a snow-covered area, or the downtown section of some large cities over which the atmosphere is polluted with visible radiation-absorbing man-made particulates, then we can see that unlike the previous situation, the intensity of the upward reflected visible radiation will decrease as the turbidity levels increase. Thus, the influence of man-made atmospheric particulate loading on the albedo, and thereby on possible surface temperature variations, serve as the motivation for the observation described in this Note.

The argument for a temperature decrease due to increasing aerosol loading is based on the exponential backscattering of particles whose minimum single scattering albedo was arbitrarily chosen to be 0.90. This value, which is low for present day global mean aerosols, implies that the absorption and backscatter fractions are equal over the visible range of wavelengths. But in fact, man-made urban particulates, which are believed to be increasing globally at a much higher rate than natural particulates (Bryson and Wendland³), have a much lower single scattering albedo. Thus, if present trends continue until man-made industrial aerosols contribute a larger percentage of the total global optical scattering centers then the mean aerosol absorption will increase and, thus, will give a much lower value for the scattering albedo, thereby possibly reversing the influence of atmospheric particulate loading from that of lowering the surface temperature of the Earth to that of increasing the temperature of the Earth.

In summary, it has been shown that local vertically integrated turbidity variations can be detected and therefore monitored by a satellite. This leads to the possibility of monitoring various molecular and particulate pollutants both on the local as well as the global scale by means of geosynchronous space stations instrumented with the proper remote sensing sounders.

References

- Risebrough, R. W., Huggett, R., Griffin, J. J., and Goldberg, E. D., "Pesticides: Transatlantic Movements in the Northeast Trades," *Science*, Vol. 159, 1968, pp. 1233–1236.
- Davitaya, F. F., "Atmospheric Dust as a Factor Affecting Glaciation and Climatic Change," *Annals Association of American Geography*, Vol. 59, 1969, pp. 552–560.
- Bryson, R. A. and Wendland, W. M., "Climatic Effects of Atmospheric Pollution," *Global Effects of Environmental Pollution*, edited by S. F. Singer, Springer-Verlag, New York, 1970, pp. 130–138.
- Bryson, R. A., "Climatic Modification by Air Pollution," International Conference on Environmental Future, Helsinki, Finland, June 27–July 3, 1971, p. 34.
- Mitchell, J. M., "Recent Secular Changes of Global Temperature," *Annals New York Academy of Science*, Vol. 95, 1961, pp. 235–250.
- Mitchell, J. M., "A Preliminary Evaluation of Atmospheric Pollution as a Cause of the Global Temperature Fluctuation of the Past Century," *Global Effects of Environmental Pollution*, edited by S. F. Singer, Springer-Verlag, New York, 1970, pp. 137–155.
- Manabe, S. and Wetherald, R. T., "Thermal Equilibrium of the Atmosphere with a Given Distribution of Relative Humidity," *Journal of Atmospheric Sciences*, Vol. 24, 1967, pp. 241–259.
- Atwater, N. A., "Planetary Albedo Changes Due to Aerosols," *Science*, Vol. 170, 1970, pp. 64–66.
- McCormick, R. A. and Ludwig, C., "Climatic Modification by Atmospheric Aerosols," *Science*, Vol. 156, 1967, pp. 1358–1359.
- Charlson, R. J. and Pilat, M. J., "Climate: the Influence of Aerosols," *Journal of Applied Meteorology*, Vol. 8, 1969, pp. 1001–1002.
- McLellan, A., "Satellite Remote Sensing of Large Scale Local Atmospheric Pollution," *Proceedings of the Second International Clean Air Congress, Washington, D.C.*, edited by H. Englund, Academic Press, New York, 1971, p. 1408.

¹² Robinson, G. D. and Drummond, A. J., "Some Recent Aircraft Measurements of the Absorption and Scattering of Solar Radiation by Atmospheric Aerosol," *Proceedings of the International Conference on Weather Modification*, AMS Boston, Mass., 1971, pp. 288-295.

¹³ McLellan, A., "Global and Local Scale Satellite Surveillance of Atmospheric Pollution," *Proceedings of the Technical Program; Electro-Optical Systems Design Conference*, Industrial and Scientific Conference Management, Inc., Chicago, Ill., 1972, pp. 244-249.

¹⁴ Darcey, R. J., "Meteorological Data Catalog for the Applications Technology Satellites, Part II," *The A.T.S. III User's Guide and Data Catalog*, Goddard Space Flight Center, Greenbelt, 1968, p. 353.

¹⁵ Sundborg, A., "Local Climatological Studies of the Temperature Conditions in an Urban Area," *Tellus*, Vol. 2, 1950, pp. 221-232.

¹⁶ Nader, J. S., ed., *Pilot Study of Ultraviolet Radiation in Los Angeles, October 1965*, U.S. Department of Health, Education, and Welfare, National Center for Air Pollution Control, Cincinnati, Ohio, 1967.

¹⁷ McCormick R. A. and Baulch, D. M., "The Variation with Height of the Dust Loading Over a City as Determined from the Atmospheric Turbidity," *Journal of Air Pollution Control Association*, Vol. 12, 1962, pp. 492-496.

¹⁸ Rasool, S. I. and Schneider, S. H., "Atmospheric Carbon Dioxide and Aerosols: Effects of Large Increases on Global Climate," *Science*, Vol. 173, 1971, pp. 138-141.

Striated Nozzle Flow with Small Radius of Curvature Ratio Throats

D. J. NORTON* AND R. E. WHITE†
Texas A&M University, College Station, Texas

Nomenclature

A, A_c = area, chamber area
 c^* = characteristic velocity
 C_p = specific heat, constant pressure
 C_D = discharge coefficient
 h, H_o = enthalpy, total enthalpy
 \dot{m} = mass flow rate
 M = Mach number
 n = curvature exponent
 P, P_o = static, total pressure
 r, z = radial, axial coordinates
 R, R_c = streamline, throat curvature
 R_T = throat radius
 T = temperature
 u, w = radial, axial velocity
 γ = isentropic exponent
 ϵ_c = contraction ratio
 ρ = density
 ψ = streamline function

Subscripts and Superscripts

g, I = gas, injector
 fu, ox = fuel, oxidizer
 i = striation zone index

Received May 1, 1973. This work was sponsored by NASA Johnson Spacecraft Center under Contract NAS 9-11658.

Index categories: Subsonic and Transonic Flow; Nozzle and Channel Flow.

* Assistant Professor, Aerospace Engineering. Member AIAA.

† Graduate Assistant, Aerospace Engineering. Student Member AIAA.

total = integrated total amount

1-D = one-dimensional

()° = reference quantity

Introduction

IN small rocket motors heat transfer can have a significant effect on engine efficiency as well as thermal protection requirements. A reduction in the heat-transfer coefficient can sometimes be accomplished by laminarization of the boundary layer using a highly convergent subsonic section and a small radius of curvature ratio throat.^{1,2} In addition to a reduction in the heat-transfer coefficient, a decrease in nozzle surface area can be achieved. Further reductions in over-all heat transfer to the nozzle walls may be effected by use of barrier cooling. In the treatment of striated flow with throat radius of curvature effects no closed form relationship exists between the chamber pressure and the mass flow. This is due to variation of total enthalpy and velocity in the chamber due to striation as well as radial pressure gradients at the physical throat due to radius of curvature effects. Thus, choking for a given throat radius can only be described and identified (and the flow parameters determined) when coupled solutions between the throat and the chamber are employed. Even for unstriated nozzle flow, the solution for the two-dimensional flowfield with small radius of curvature ratio throats is difficult and time consuming.³ When designing rocket motors a rapid means of estimating the performance of a motor with barrier cooling and for sharp throats is therefore desirable to permit the evaluation of potential designs.

Analysis

Since the throat solution is coupled to the chamber solution, it is also necessary to establish the relationship between the injection scheme and the throat. Figure 1a presents the flow regimes of interest in which mass, momentum, and energy

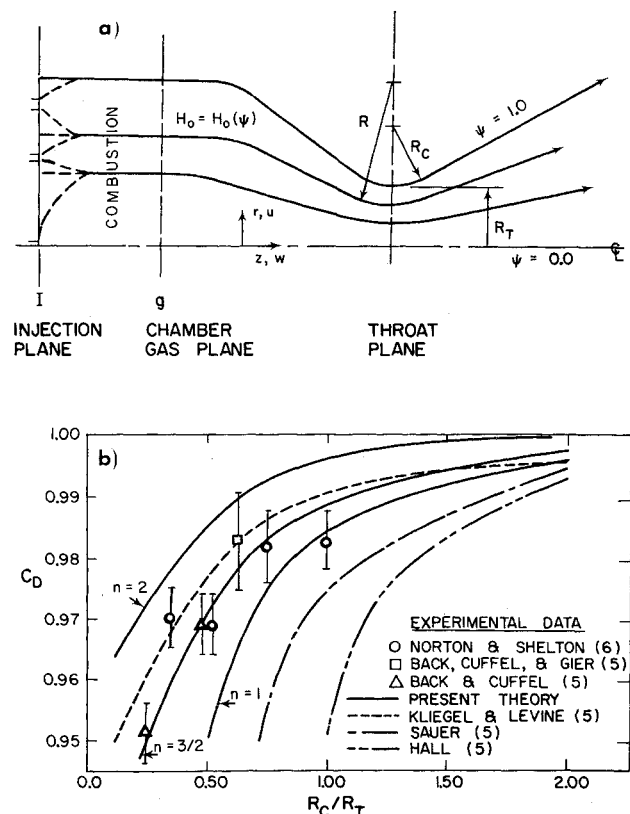


Fig. 1 a) Nozzle schematic and flow geometry; b) theoretical and experimental results for C_D vs R_c/R_T .